

Electromagnetic Fields Simulating a Rotating Sphere and its Exterior

Daniele Funaro

Dipartimento di Scienze Chimiche e Geologiche
Università di Modena e Reggio Emilia
Via Campi 103, 41125 Modena (Italy)
daniele.funaro@unimore.it

Abstract

Vector displacements expressed in spherical coordinates are proposed. They correspond to electromagnetic fields in vacuum that globally rotate about an axis and display many circular patterns on the surface of a sphere. The fields basically satisfy the set of Maxwell's equations, but enjoy further properties that allow them to be suitably interpreted as solutions of a plasma model that combines electrodynamics with the Euler's equation for fluids. Connection with magnetohydrodynamics can also be established. The fields are extended with continuity outside the sphere in a very peculiar manner. In order to avoid peripheral velocities of arbitrary magnitude, as it may happen for a rigid rotating body, they are organized to form successive encapsulated shells, with substructures recalling successive ball-bearing assemblies. A recipe for the construction of these solutions is provided by playing with the eigenfunctions of the vector Laplace operator. Some applications relative to astronomy are finally discussed.

Keywords: exact solutions; electrodynamics; eigenfunctions; Bessel functions; associated Legendre polynomials.

AMS classification: 33C47, 35Q61, 78A25.

1 Forewords

The main practical achievement of this paper is the introduction of new exact solutions for a set of equations modeling electrodynamics. The result has by itself a general validity and can be applied in many circumstances emerging in the context of electromagnetism (EM), magnetohydrodynamics (MHD), or geophysics. It may also represent a referring point to develop alternative numerical type simulations, especially in the context of spectral type approximation methods.

The fields are described in spherical coordinates and solve the whole set of Maxwell's equations in vacuum. They are obtained by separation of variables. As usual, this procedure leads to trigonometric functions for the azimuthal angle and Bessel's functions for the radial component. As far as the altitude angle is concerned, one obtains a family of special functions that can be put in connection with the so called *Associated Legendre polynomials*. The proposed setting is not directly related to the family of *vector spherical harmonics*. The new fact here is that the displacement rigidly rotates about an axis at speeds comparable to that of light, with an angular velocity depending on a parameter ω . The set up of the equations and the structure of the solutions is given in section 2. In the successive sections 3 and 4, explicit computations are carried out to check that the vector fields actually satisfy all the equations.

We also worked on the possibility to prolong the electromagnetic fields outside a given sphere. Since the solutions are defined in the whole tridimensional space, a natural extension already exists. Nevertheless, such a straightforward expansion would bring to peripheral velocities of arbitrary magnitude, which is unphysical. The question is however well-posed, since the dynamical fields present on the sphere surface may be used as boundary constraints to analyze the external problem. Such a study is approached in [22], section 89, from the relativistic viewpoint. Here, due to the lack of space, we will not touch on questions pertaining to general relativity, although the argument is very appropriate.

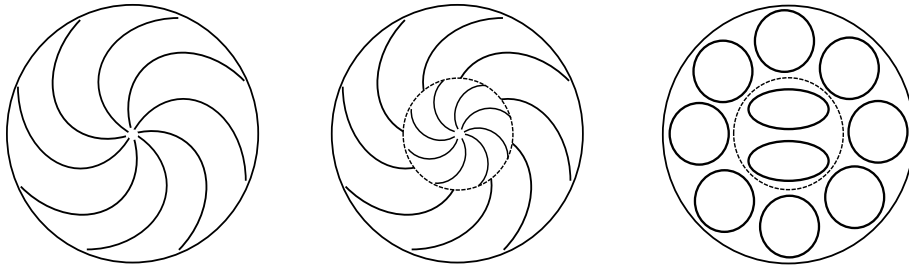


Figure 1: Due to the boundedness of the speed of light, the spiraling patterns of the left picture, tend to break up after a certain time (central picture). In our approach (right), a fast rotating core induces the rotation of an external one with a lower angular velocity. Differently from the previous case, this transfer can be done with continuity.

Because of the boundedness of the speed of light, as we move away from a central core, the rotatory information produces a spiral as in the first picture of Fig. 1. Nevertheless, we guess that this behavior cannot be maintained for long times and sooner or later a breakdown occurs. Such a phenomenon recalls that characterizing tornados, where a high-frequency whirl becomes isolated and drags the outside air to turn around at lower frequency (secondary vortex). This is essentially due to the limits imposed by the speed of sound in air and by

viscosity. We would like to reproduce a situation where the rotating sphere is surrounded by another EM configuration evolving at lower angular velocity. The process may be repeated, so producing a sequence of encapsulated environments. The most important achievement is that the connections can be done by avoiding discontinuities. This brings us to the third picture of Fig. 1, and to Fig. 5. We postpone the discussion of the main idea to section 5, by showing how this can be quantitatively implemented.

In section 6, we add stationary fields to the dynamical solutions examined so far, and we examine the possible links with some model equations arising from the study of plasma. Finally, section 7 is devoted to some speculative considerations about the constitution of the Sun and the corresponding solar system, that descend as a natural consequence of the analytic construction.

2 Preliminary setting

We start by introducing the classical Maxwell's equations in vacuum. We denote by $\mathbf{E} = (E_1, E_2, E_3)$ the electric field and by $\mathbf{B} = (B_1, B_2, B_3)$ the magnetic field. We first have the Ampère's law, with no current source term:

$$\frac{\partial \mathbf{E}}{\partial t} = c^2 \text{curl} \mathbf{B} \quad (1)$$

where c is the speed of light. Successively, we have the Faraday's law:

$$\frac{\partial \mathbf{B}}{\partial t} = - \text{curl} \mathbf{E} \quad (2)$$

Finally, we close the set with the following conditions on the divergence:

$$\text{div} \mathbf{E} = 0 \quad (3)$$

$$\text{div} \mathbf{B} = 0 \quad (4)$$

It is well known that, by suitably combining the equations (1), (2), (3), (4), it is not difficult to arrive at the vector wave equations:

$$\frac{\partial^2 \mathbf{E}}{\partial t^2} = c^2 \Delta \mathbf{E} \quad \frac{\partial^2 \mathbf{B}}{\partial t^2} = c^2 \Delta \mathbf{B} \quad (5)$$

It is standard to introduce the electromagnetic potentials $\mathbf{A} = (A_1, A_2, A_3)$ and Φ , such that:

$$\mathbf{B} = \frac{1}{c} \text{curl} \mathbf{A} \quad \mathbf{E} = - \frac{1}{c} \frac{\partial \mathbf{A}}{\partial t} - \nabla \Phi \quad (6)$$

By assuming this, equations (2) and (4) are automatically satisfied. The potentials are not unique, but are usually related through some gauge condition. For convenience, the Lorenz's gauge will be assumed:

$$\text{div} \mathbf{A} + \frac{1}{c} \frac{\partial \Phi}{\partial t} = 0 \quad (7)$$

We work in spherical coordinates (r, θ, ϕ) . Hereafter $H = H(r)$ will denote a function of the variable r , whereas S_2, S_3 will be functions of the variable $x = \cos \theta$. We also set $\zeta = c\omega t - m\phi$, where $\omega > 0$ is a parameter. This setting allows us to simulate the motion of an EM wave rotating around the vertical axis (orthogonal to the equatorial plane $\theta = \pi/2$). We then look for magnetic fields of the form:

$$\mathbf{B}_D = (B_1, B_2, B_3) = \frac{1}{c} \left(0, H(r)S_2(\cos \theta) \cos \zeta, H(r)S_3(\cos \theta) \sin \zeta \right) \quad (8)$$

Thus, we have: $B_1 = 0$. The expression in (8) is required to satisfy the condition $\text{div} \mathbf{B}_D = 0$ as well as the wave equation in (5). This is possible for special choices of the functions H, S_2, S_3 . The results of this tedious analysis are reported in the next sections. The subscript D stands for *Dynamical*, to distinguish the present field from the *Stationary* one \mathbf{B}_S that will be introduced later on.

Regarding the electric field, it is enough to take the *curl* of \mathbf{B}_D and integrate with respect to time (see (1)). This yields:

$$\begin{aligned} \mathbf{E}_D = (E_1, E_2, E_3) = \frac{1}{\omega} \left(\frac{H}{r} \sqrt{1-x^2} \left[S_3' - \frac{x}{1-x^2} S_3 + \frac{m}{1-x^2} S_2 \right] \cos \zeta, \right. \\ \left. \left(H' + \frac{H}{r} \right) S_3 \cos \zeta, \left(H' + \frac{H}{r} \right) S_2 \sin \zeta \right) \end{aligned} \quad (9)$$

where S_3 is differentiated with respect to x , and H with respect to r . Another equivalent version of (9) is found in (30). It is a rather boring exercise to check that $\rho_D = \text{div} \mathbf{E}_D = 0$ and that the electric field satisfies the vector wave equation. It is interesting to point out that in general $\mathbf{E}_D \cdot \mathbf{B}_D \neq 0$, providing an example of solutions of Maxwell's equations where electric and magnetic fields are not orthogonal. Note that, at the radial points where $H = 0$, we obtain that $\mathbf{B}_D = 0$ and that \mathbf{E}_D is tangential to the sphere. The distribution of the electric field in correspondence of these points is displayed in Fig. 3. As far as we know, the type of rotating waves we are examining here are not related to the family of *Vector Spherical Harmonics*. Similarities can be found with the eigenvalues of the *Laplace's tidal equation* (see [23]). The literature offers plenty of results regarding the eigenmodes of the scalar Laplace equation in spherical coordinates, but very few for the vector version. Alternative solutions, naturally embedded in toroid shaped regions, are explicitly found in [8] and [15].

We can define the electromagnetic potentials by setting $\Phi_D = 0$ and recovering \mathbf{A}_D by integrating \mathbf{E}_D in time. In this way the second relation in (6) is fulfilled. Since $\text{div} \mathbf{A}_D = 0$ we are in the Lorenz's gauge. One can verify that also the first relation in (6) is satisfied.

We conclude this section by defining the velocity vector field:

$$\mathbf{V} = \left(0, 0, \frac{c\omega}{m} r \sin \theta \right) \quad (10)$$

which actually simulates a uniform rotation around the vertical axis. An important relation that will be used later on is the following one (see section 2 for

the proof):

$$\mathbf{E}_D + \mathbf{V} \times \mathbf{B}_D = -\nabla p_D \quad \text{with} \quad p_D = -\frac{1}{m\omega}(rH' + H)S_2 \sin \theta \cos \zeta \quad (11)$$

This allows us to introduce a new potential p_D . Another solution, with the same properties of the one just examined is found in [12], p. 147. Let us observe that in the homogeneous Maxwell's equations the role of \mathbf{E}_D and \mathbf{B}_D can be interchanged. This is not true anymore if we want to preserve the additional property (11).

3 Explicit computation

We first check that \mathbf{B}_D , as defined in (8), has zero divergence and satisfies the vector wave equation (5). More exactly, we show that:

$$\frac{\partial^2 \mathbf{B}_D}{\partial t^2} = -c^2 \omega^2 \mathbf{B}_D \quad \Delta \mathbf{B}_D = -\omega^2 \mathbf{B}_D \quad (12)$$

The symbol Δ denotes the vector Laplacian in spherical coordinates. We recall that S_2 and S_3 are functions of $x = \cos \theta$. Since $B_1 = 0$, we must have:

$$\begin{aligned} \operatorname{div} \mathbf{B}_D &= \frac{1}{r \sin \theta} \left[\frac{\partial}{\partial \theta} (B_2 \sin \theta) + \frac{\partial B_3}{\partial \phi} \right] \\ &= \frac{H}{cr \sin \theta} \left[\frac{d}{d\theta} (S_2 \sin \theta) - mS_3 \right] \cos \zeta = 0 \end{aligned} \quad (13)$$

Next, the following relations hold:

$$\frac{dS_2}{d\theta} = -S_2'(x)\sqrt{1-x^2} \quad \frac{d^2 S_2}{d\theta^2} = S_2''(x)(1-x^2) - xS_2'(x) \quad (14)$$

where the prime denotes the derivative with respect to x . Thus, the divergence is zero everywhere if and only if:

$$\frac{d}{d\theta} (S_2 \sin \theta) - mS_3 = -(1-x^2)S_2' + xS_2 - mS_3 = 0 \quad (15)$$

which is equivalent to:

$$mS_3 = -(1-x^2)S_2' + xS_2 = -\sqrt{1-x^2} \left(S_2 \sqrt{1-x^2} \right)' \quad (16)$$

We can then differentiate the above expression obtaining:

$$mS_3' = -(1-x^2)S_2'' + 3xS_2' + S_2, \quad mS_3'' = -(1-x^2)S_2''' + 5xS_2'' + 4S_2' \quad (17)$$

As far as the eigenvalue problem in (12) (second equation) is concerned, we observe that the first component of $\Delta \mathbf{B}_D$ is automatically zero by virtue of (13):

$$(\Delta \mathbf{B}_D)_1 = -\frac{2}{r^2 \sin \theta} \left[\frac{\partial}{\partial \theta} (B_2 \sin \theta) + \frac{\partial B_3}{\partial \phi} \right] = 0 \quad (18)$$

Regarding the two other components, we have:

$$c(\Delta \mathbf{B}_D)_2 = \left(H'' + \frac{2H'}{r} \right) S_2 \cos \zeta + \frac{H}{r^2} \cos \zeta \left[\frac{1}{\sin \theta} \frac{d}{d\theta} \left(\sin \theta \frac{dS_2}{d\theta} \right) - \frac{m^2 + 1}{\sin^2 \theta} S_2 + \frac{2m \cos \theta}{\sin^2 \theta} S_3 \right] \quad (19)$$

$$c(\Delta \mathbf{B}_D)_3 = \left(H'' + \frac{2H'}{r} \right) S_3 \sin \zeta + \frac{H}{r^2} \sin \zeta \left[\frac{1}{\sin \theta} \frac{d}{d\theta} \left(\sin \theta \frac{dS_3}{d\theta} \right) - \frac{m^2 + 1}{\sin^2 \theta} S_3 + \frac{2m \cos \theta}{\sin^2 \theta} S_2 \right] \quad (20)$$

where here the prime denotes the derivative with respect to r .

We now require H to satisfy the eigenvalue problem:

$$H'' + \frac{2H'}{r} - \ell(\ell + 1) \frac{H}{r^2} = -\omega^2 H \quad (21)$$

The above equation leads us to spherical Bessel's functions. Therefore, we have the linear combination of these expressions:

$$H(r) = \sqrt{\frac{\pi}{2\omega r}} J_{\ell+1/2}(\omega r) \quad H(r) = \sqrt{\frac{\pi}{2\omega r}} Y_{\ell+1/2}(\omega r) \quad (22)$$

where J_α is the Bessel's function of the first kind and Y_α is that of the second kind. Note that the last one is singular for $r = 0$. Note also that, for the moment, ℓ does not necessitate to be an integer.

By imposing that $\Delta \mathbf{B}_D = -\omega^2 \mathbf{B}_D$, using (16) and translating as a function of the variable x the term in brackets of (19), we arrive at:

$$(1 - x^2)S_2'' - 4xS_2' - \frac{m^2 - 1}{1 - x^2}S_2 + [\ell(\ell + 1) - 2]S_2 = 0 \quad (23)$$

which is the equation to be satisfied by S_2 . A discussion of the eigenvalue problem (23) is given in section 4. We can argue with (20) in a similar way, obtaining:

$$(1 - x^2)S_3'' - 2xS_3' - \frac{m^2 + 1}{1 - x^2}S_3 + \ell(\ell + 1)S_3 + \frac{2mx}{1 - x^2}S_2 = 0 \quad (24)$$

The above equation relates S_2 and S_3 . We must observe at this point that a relation between S_2 and S_3 has been already set up through (16). We have to check that these two are equivalent. To this end, we differentiate (23) with respect to x :

$$(1 - x^2)S_2''' - 6xS_2'' - \frac{m^2 - 1}{1 - x^2}S_2' - \frac{2(m^2 - 1)x}{(1 - x^2)^2}S_2 + [\ell(\ell + 1) - 6]S_2' = 0 \quad (25)$$

Using (16) we rewrite (24) in terms of the sole unknown S_2 , which appears with its third derivative S_2''' . This last is replaced by that recovered from (25), in order to get a second order differential equation. After tedious simplifications one discovers that this last equation is nothing but (23) multiplied by x . Hence, by assuming that both (16) and (23) are true, we actually verify (24), showing that $(\Delta \mathbf{B}_D)_3 = -\omega^2 B_3$ is automatically satisfied when $\text{div} \mathbf{B}_D = 0$ and $(\Delta \mathbf{B}_D)_2 = -\omega^2 B_2$ hold true. We can finally claim that the wave equation for \mathbf{B}_D is satisfied when H comes from (21), S_2 comes from (23), and S_3 is chosen as in (16).

As a final exercise we check (11). We start by writing:

$$\mathbf{V} \times \mathbf{B}_D = -\frac{\omega}{m} \left(HrS_2 \sin \theta \cos \zeta, 0, 0 \right) \quad (26)$$

We have to prove that:

$$-\nabla p_D = -\left(\frac{\partial p_D}{\partial r}, \frac{1}{r} \frac{\partial p_D}{\partial \theta}, \frac{1}{r \sin \theta} \frac{\partial p_D}{\partial \phi} \right) = \left((\mathbf{E}_D + \mathbf{V} \times \mathbf{B}_D)_1, E_2, E_3 \right) \quad (27)$$

The verification is straightforward for the second and the third components. Concerning the first one, we begin with noting that:

$$\begin{aligned} \ell(\ell+1)S_2 &= -(1-x^2)S_2'' + 4xS_2' + \frac{m^2-1}{1-x^2}S_2 + 2S_2 \\ &= m \left[S_3' - \frac{x}{1-x^2}S_3 + \frac{m}{1-x^2}S_2 \right] \end{aligned} \quad (28)$$

where we used (23), the first equation in (17), and (16). The last term above is equal to the one in square brackets in (9). We finally have:

$$\begin{aligned} -\frac{\partial p_D}{\partial r} &= \frac{1}{m\omega} (rH'' + 2H')S_2 \sin \theta \cos \zeta = \frac{H}{m\omega} \left(\frac{1}{r} \ell(\ell+1) - \omega^2 r \right) S_2 \sin \theta \cos \zeta \\ &= \frac{H}{m\omega r} \ell(\ell+1)S_2 \sin \theta \cos \zeta + (\mathbf{V} \times \mathbf{B}_D)_1 = (\mathbf{E}_D + \mathbf{V} \times \mathbf{B}_D)_1 \end{aligned} \quad (29)$$

where we used (21). This completes the proof of (27).

By virtue of (28), we can rewrite (9) as follows:

$$\mathbf{E}_D = \frac{1}{\omega} \left(\frac{H}{rm} \ell(\ell+1)S_2 \sin \theta \cos \zeta, \left(H' + \frac{H}{r} \right) S_3 \cos \zeta, \left(H' + \frac{H}{r} \right) S_2 \sin \zeta \right) \quad (30)$$

4 Further insight

Here, we would like to examine the properties of equation (23). As a particular example, we start by studying the case $m=1$, where $\zeta = c\omega t - \phi$. In this situation the set of solutions is well characterized. Up to multiplicative constants, it consists of the set of Jacobi polynomials $P_\ell^{(1,1)}$, where ℓ is integer and denotes

the degree. For instance, by taking $\ell = 1$, we get $S_2(x) = 1$ and $S_3(x) = x$. In this simple situation the vector potential takes the form:

$$\mathbf{A}_D = -\frac{1}{\omega^2} \left(\frac{2}{r} H \sin \theta \sin \zeta, \left(H' + \frac{H}{r} \right) \cos \theta \sin \zeta, -\left(H' + \frac{H}{r} \right) \cos \zeta \right) \quad (31)$$

where H satisfies:

$$H'' + \frac{2H'}{r} - \frac{2H}{r^2} = -\omega^2 H \quad (32)$$

having for solution a linear combination of the two following Bessel's functions:

$$\sqrt{\frac{\pi}{2\omega r}} J_{3/2}(\omega r) = \frac{\sin \omega r}{(\omega r)^2} - \frac{\cos \omega r}{\omega r}, \quad \sqrt{\frac{\pi}{2\omega r}} Y_{3/2}(\omega r) = -\frac{\cos \omega r}{(\omega r)^2} - \frac{\sin \omega r}{\omega r} \quad (33)$$

Note that the vector representing the magnetic field \mathbf{B}_D at the poles ($\theta = 0$ or $\theta = \pi$) is tangent to the sphere and rotates with angular velocity $c\omega$. This will not be true for $m > 1$, where \mathbf{B}_D is going to be zero at the poles.

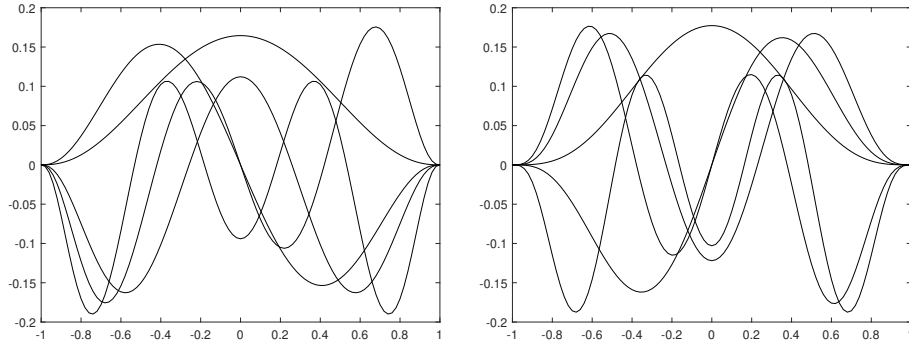


Figure 2: Eigensolutions of (23) for $m = 6$, $\ell = 6, 7, 8, 9, 10$ (left) and $m = 8$, $\ell = 8, 9, 10, 11, 12$ (right).

We did not find documentation for a general $m > 1$, but we presume that the problem has been already studied. The situation is very similar to that related to the so called *Associated Legendre polynomials* (see e.g. [1], p. 331), where the term $-m^2/(1-x^2)$ is added to the classical differential operator $(1-x^2)(d^2/dx^2) - 2x(d/dx)$. Here the operator is slightly different, i.e.: $(1-x^2)(d^2/dx^2) - 4x(d/dx)$. Connections with the so called Hough functions may be devised (see, e.g.: [37]). The results of some numerical computations show that the eigenvalue problem:

$$(1-x^2)S'' - 4xS' - \frac{m^2-1}{1-x^2}S = -\lambda S \quad (34)$$

is actually solvable. The values of λ exactly correspond to numbers of the form $[\ell(\ell+1)-2]$, where ℓ is integer with $\ell \geq m$. For a fixed $m > 1$ the eigenfunctions

increase their frequency as ℓ grows. Differently from the case $m = 1$, they satisfy homogeneous boundary conditions at the points ± 1 (the poles of the sphere). Some plots are given in Fig. 2. The eigenfunctions are orthogonal with respect to the inner product of the space $L_w^2(-1, 1)$, weighted by the function $w = 1 - x^2$. A similar orthogonality relation holds for the derivatives. In particular, if S and T are solutions of (23) corresponding to different values of ℓ , we have:

$$\int_{-1}^1 ST(1 - x^2)dx = 0, \quad \int_{-1}^1 S'T'(1 - x^2)^2dx + (m^2 - 1) \int_{-1}^1 STdx = 0 \quad (35)$$

The distribution of the electromagnetic fields is rather complicated. We can examine the case of a sphere having the radius corresponding to a zero of H (recall that H is related to Bessel's functions, so that it displays infinite zeros). By looking at (8) and (9), we easily realize that \mathbf{B}_D is identically zero on the surface of that sphere, whereas \mathbf{E}_D turns out to be tangential and organized to form several vortices. The number of vortices along the azimuthal direction is ruled by the parameter m . The number of vortices spanned by the altitude angle depends on ℓ . A typical configuration is displayed in Fig. 3. The displacement rotates about the vertical axis, as prescribed by the velocity field \mathbf{V} . Similar conclusions can be made for \mathbf{B}_D when the radius of the sphere is not equal to a zero of H .

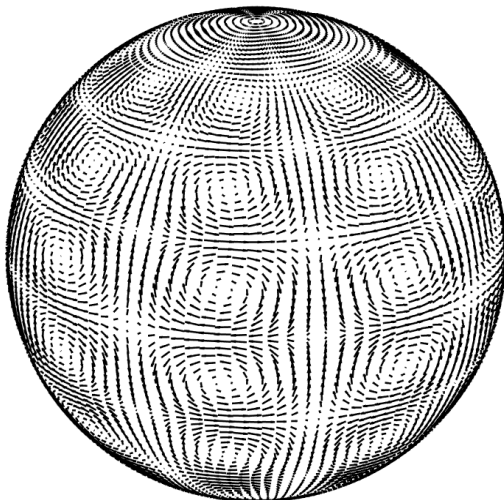


Figure 3: Electric field distribution on the surface of a sphere having the radius corresponding to a zero of the function H . In this situation, the magnetic field is uniformly zero. The number of vortices depends on the parameters. In the present case we have: $m = 4$ and $\ell = 11$.

An explicit solution for $m = \ell \geq 1$ is known. This is given by setting:

$$S_2(\cos \theta) = (\sin \theta)^{m-1} \quad S_3(\cos \theta) = \cos \theta (\sin \theta)^{m-1} \quad (36)$$

With the help of (36) we can better examine the distribution of the fields in the case $m = \ell = 2$. For $H \neq 0$, we get from (8):

$$\mathbf{B}_D = \frac{H(r)}{c} (0, \sin \theta \cos \zeta, \sin \theta \cos \theta \sin \zeta) \quad (37)$$

For $H = 0$, we get instead from (9):

$$\mathbf{E}_D = \frac{H'(r)}{\omega} (0, \sin \theta \cos \theta \cos \zeta, \sin \theta \sin \zeta) \quad (38)$$

The corresponding electric and magnetic fields are respectively shown in Fig. 4.

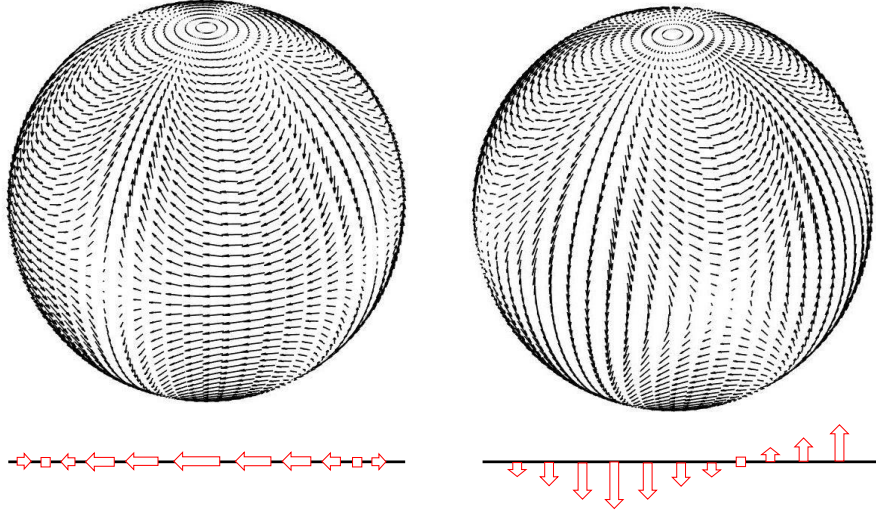


Figure 4: Field distributions: electric (left) for radial points where $H = 0$; magnetic (right) for radial points where $H \neq 0$. Both pictures refer to the situation $m = \ell = 2$. At the equator, the electric field oscillates horizontally, whereas the magnetic field is lined up with the meridians.

5 Extension outside the sphere

We continue our exploration on the solutions (8) and (9) in the special case where $m = \ell$. We examine what happens outside the sphere. The expressions in (36) tell us that, for large m , the function S_2 assumes the value 1 for $\theta = \pi/2$ and goes fast to zero as approaching $\theta = 0$ or $\theta = \pi$. The fields are then

concentrated in a flat annular region around the equator. As reported in Fig. 4, for $H = 0$, the electric field is lined up with the equator and oscillates according to the rule $\cos \zeta = \cos(c\omega t - m\phi)$. For $H \neq 0$, the magnetic field follows the same behavior, but it is oriented as the meridians. Based on (10), at a radius r , the intensity of the peripheral velocity of this equatorial wave is $V(r) = c\omega r/m$.

As r reaches a zero of H , the magnetic field vanishes. We believe that in this circumstance there is a change of regime. In fact, it is difficult to accept the idea that, by increasing r , the quantity $V(r)$ is allowed to assume any possible value, as it would be for a rotating rigid body in classical mechanics. It is reasonable to guess instead that $V(r)$ does not exceed too much the speed of light in vacuum. This is thinkable if we suppose that the process happens through some quantized steps. Indeed, it is possible to build encapsulated shells. Inside each one of them we are solving a wave type equation. The angular velocity decreases by passing from a shell to an external one. Moreover, such a passage can be made in continuous way. We show how this extraordinary fact can be achieved.

We adapt to the present circumstances a situation already studied in [13]. The aim is to construct solutions defined on a circular crown, in such a way that the velocity at the internal boundary is more or less the same (in magnitude) than that at the external boundary. This construction relies on the possibility to find eigenfunctions of the Laplace operator, corresponding to eigenvalues of multiplicity four, at least. Technically, the question is reduced to find suitable periodic solutions of the wave equations (5). After separation of variables and further simplifications ($m = \ell$), the problem can be studied for a scalar equation in two dimensions, but the general discussion in 3D involves the same ingredients. The domain is an annular region between the radii r_{\min} and r_{\max} . Homogeneous Dirichlet boundary conditions are assumed, though such a constraint is not strict. The solution must develop in such a way that, in proximity of the inner boundary, the shift is governed by the rule $\cos(c\omega t - m_A\phi)$, where m_A is an integer. At the outside boundary we should have instead $\cos(c\omega t - m_B\phi)$, where $|m_B| > |m_A|$ is another integer. At these boundaries, the velocity of rotation is expressed by (10). If the rotating body was rigid, the external velocity would be larger than the internal one, directly depending on the ratio r_{\max}/r_{\min} . Here we can play instead with the values of the integers m_A and m_B , in order to obtain that the intensity of the inner velocity $c\omega r_{\min}/m_A$ is comparable with the external one $c\omega r_{\max}/m_B$.

Such an analysis is not trivial and passes through the determination of the zeros of the Laplacian eigenfunctions in the domain. In fact, not all the configurations are possible. The parameters to play with are: m_A , m_B , ω and r_{\max}/r_{\min} . They have to be detected in order to have a basis of at least four orthogonal eigenfunctions corresponding to the same eigenvalue (which, as a consequence, must have multiplicity equal to 4). Interesting dynamical patterns are then obtained from suitable linear combinations of these eigenfunctions.

The underlying idea of this construction is to recreate something similar to an interconnected set of gears of different size: the small one turning fast, imparts a slow rotation to the big one. The case of an annular region is better described by a ball bearing assembly (see Fig. 5), where, in smooth way, the

momentum of the internal support is transferred to the external one, avoiding the inconveniences (and the paradoxes) related to the rotation of a rigid body.

From the practical viewpoint, let r_{\min} denote the interior radius of the annulus. By recalling (22), we define the following function:

$$F_m(r) = \frac{1}{\sqrt{\omega r}} \left(Y_{m+\frac{1}{2}}(\omega r_{\min}) J_{m+\frac{1}{2}}(\omega r) - J_{m+\frac{1}{2}}(\omega r_{\min}) Y_{m+\frac{1}{2}}(\omega r) \right) \quad (39)$$

It is easy to check that: $F_m(r_{\min}) = 0$.



Figure 5: Ball bearing assembly. In the referring frame where the spheres are at rest, the internal and the external boundaries counter rotate, displaying different angular velocities. A similar effect can be achieved by solving the wave equation in a suitable annular region. In this circumstance, the size and the frequencies involved must be wisely calibrated.

We would like now to find two different integers m_A and m_B , a value of the parameter ω , and a radius r_{\max} of the external circumference of the annulus. This has to be done in order to satisfy the conditions:

$$F_{m_A}(r_{\max}) = 0, \quad F_{m_B}(r_{\max}) = 0 \quad (40)$$

The explanation is as follows. We require homogeneous Dirichlet conditions on the boundaries of the annulus (internal and external), and we want this to be simultaneously achieved for different frequencies m_A and m_B . Such a problem does not always admit solution. Possible allowed combinations (among infinite others) for $r_{\min} = 1$ are: $m_A = 2, m_B = 5, \omega \approx 1.97, r_{\max} \approx 4.75$; $m_A = 2, m_B = 6, \omega \approx 3.72, r_{\max} \approx 2.83$; or $m_A = 2, m_B = 8, \omega \approx 2.39, r_{\max} \approx 5.35$. The last case is represented in Fig. 6.

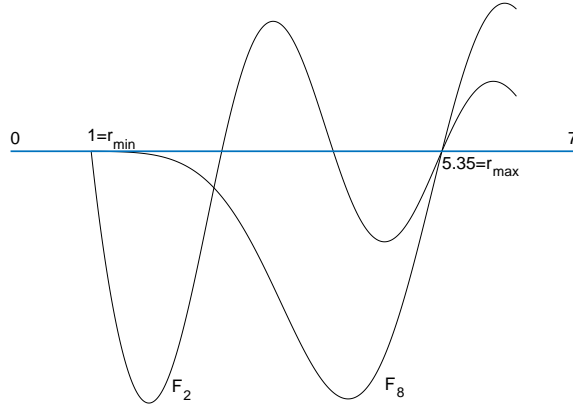


Figure 6: Both the two functions F_2 and F_8 vanish at $r_{\min} = 1$ and $r_{\max} \approx 5.35$. The amplitude of the functions have been suitably rescaled to make more clear the graphical output.

Reminding once again that we are examining the case $m = \ell$ (see also (36)), the expression in (39) has a link with the eigenfunctions studied so far, where the dependence from the variable θ is neglected. We can actually define:

$$\Phi_m(r, \phi) = \alpha_m F_m(r) \cos(m\phi) \quad \Psi_m(r, \phi) = \beta_m F_m(r) \sin(m\phi) \quad (41)$$

for arbitrary multiplicative constants α_m and β_m . By restoring the part in the variable θ , these are indeed two orthogonal eigenfunctions with eigenvalue $-\omega^2$. We get solutions of the wave equation by introducing combinations depending on time. For different values of m_A and m_B , we can write:

$$\Phi_{m_A} \sin(c\omega t) + \Phi_{m_B} \cos(c\omega t) + \Psi_{m_A} \sin(c\omega(t + t_0)) + \Psi_{m_B} \cos(c\omega(t + t_0)) \quad (42)$$

where t_0 is a time shift.

By suitably adjusting t_0 , α_m and β_m , we get interesting evolution patterns. This is the case for instance of the plots of Fig. 7, where $m_A = 2$, $m_B = 8$, $\omega \approx 2.39$ and $r_{\max}/r_{\min} = 5.35$. The combination of Φ_2 and Ψ_2 gives origin to the part of the solution that rotates with azimuth $\zeta = c\omega t - 2\phi$ and internal velocity $c\omega r_{\min}/2 \approx 1.2c$. Similarly, the part related to Φ_8 and Ψ_8 counter rotates with azimuth $\zeta = c\omega t + 8\phi$ and external velocity $c\omega r_{\max}/8 \approx 1.6c$. Note that if the body was rigid, the external velocity would have been approximately equal to $6.4c$, exaggeratedly exceeding the speed of light. Another example of this type is shown in Fig. 5, where the parameters are $m_A = 4$, $m_B = 20$, $\omega \approx 13$ and $r_{\max}/r_{\min} \approx 2$. Here the external velocity is even lower than the internal one. These plots can be however fully understood and appreciated only with the help of animations.

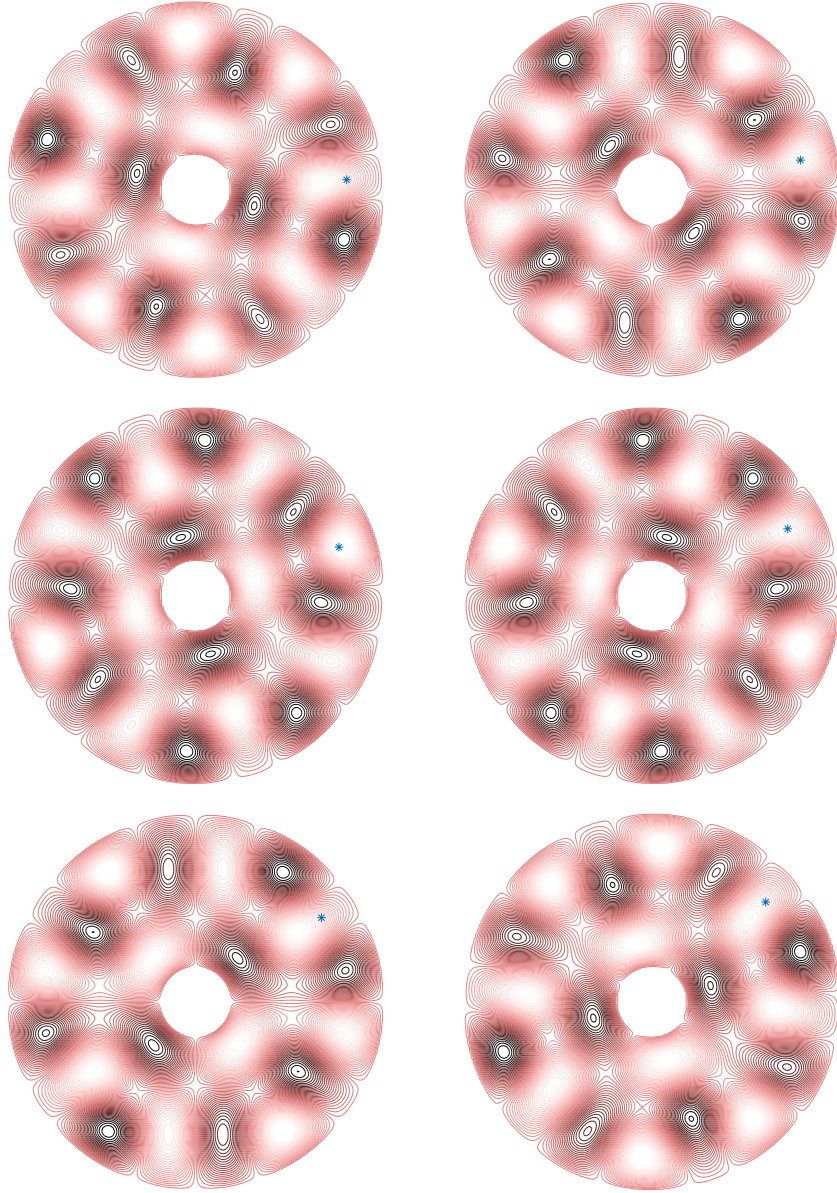


Figure 7: Solution of the wave equation for a period of time. As the central core makes a half clock-wise rotation, the peripheral part accomplishes an eighth of a cycle in anti clock-wise manner, as testified by the position of the asterisk.

6 Validity in a more extended context

By a suitable merging of the classical electrodynamics equations with those ruling inviscid fluids, a revision of the theory of EM in vacuum has been proposed in [12] and successively developed in [14]. Such an alternative model strictly includes the subspace of solutions of the classical Maxwell's equations, so that it allows for the study of a larger variety of electromagnetic phenomena. The main extension is the possibility to deal with situations where the divergence of the electric field is different from zero, even if actual charges are not present (as electrons or positive nuclei). An important motivation in favor of the revised model relies on the possibility to build compact solutions (solitary waves) traveling undisturbed without dissipation (see (62)).

We can find many arguments to support the fact that the wave equation for \mathbf{E} and the divergence-free condition $\text{div}\mathbf{E} = 0$ cannot hold, in general, at the same time. The most trivial one is that, in order to get (5) we must use $\text{div}\mathbf{E} = 0$, since $\text{curl}(\text{curl}\mathbf{E}) = -\Delta\mathbf{E} + \nabla(\text{div}\mathbf{E})$. On the other hand, mathematically, any vector wave equation, furnished with initial and boundary conditions (imposed in a quite arbitrary manner), has unique solution. The chances that such a solution has (in addition) zero divergence, are rather limited. A fast movement of charged bodies may actually create regions in the intermediate vacuum, where $\text{div}\mathbf{E} \neq 0$.

The revised set of equations reads as follows (check the similarity with those given for instance in [19], p. 491, concerning the modeling of plasmas):

$$\frac{\partial\mathbf{E}}{\partial t} = c^2\text{curl}\mathbf{B} - \rho\mathbf{V} \quad (43)$$

$$\frac{\partial\mathbf{B}}{\partial t} = -\text{curl}\mathbf{E} \quad (44)$$

$$\text{div}\mathbf{B} = 0 \quad (45)$$

$$\rho\left(\frac{D\mathbf{V}}{Dt} + \mu(\mathbf{E} + \mathbf{V} \times \mathbf{B})\right) = -\nabla p \quad (46)$$

where we defined $\rho = \text{div}\mathbf{E}$, and:

$$\frac{D\mathbf{V}}{Dt} = \frac{\partial\mathbf{V}}{\partial t} + (\mathbf{V} \cdot \nabla)\mathbf{V} \quad (47)$$

Relation (46) is the Euler's equation for the velocity field \mathbf{V} , provided with a forcing term of EM type given by the vector: $\mathbf{E} + \mathbf{V} \times \mathbf{B}$. The Maxwell's case in vacuum is now recovered by imposing $\rho = 0$ and $p = 0$. Therefore, the new set of equations is actually an extension of the classical model. The case when $D\mathbf{V}/Dt = 0$ and $p = 0$ will be mentioned later in this section.

Dimensionally, the constant μ is charge divided by mass. In Appendix H in [14] is estimated to be approximately equal to 2.85×10^{11} Coulomb/Kg, which is more or less of the same order of magnitude of the elementary charge divided by the electron mass. Up to dimensional scaling, the scalar p plays the role of

pressure. Indeed, the quantity $(\epsilon_0/\mu)p$ (where ϵ_0 is the dielectric constant in vacuum) is dimensionally equivalent to a force per unity of surface.

A further equation, related to energy conservation arguments, is finally added:

$$\frac{\partial p}{\partial t} = \mu\rho \mathbf{E} \cdot \mathbf{V} \quad (48)$$

This says that pressure may come into place as a consequence of a lack of orthogonality between \mathbf{E} and \mathbf{V} . This is definitely what happens to the fields introduced in the previous sections.

By taking the divergence of (43), it is straightforward to get the following continuity equation:

$$\frac{\partial \rho}{\partial t} + \text{div}(\rho\mathbf{V}) = 0 \quad (49)$$

Thus, the above relation is a consequence of the model and does not represent an extra requirement. Finally, by scalar multiplication of (46) by \mathbf{V} and by taking into account (48), we arrive at a Bernoulli's type equation:

$$\frac{\rho}{2} \frac{D|\mathbf{V}|^2}{Dt} + \frac{Dp}{Dt} = 0 \quad (50)$$

Since the EM fields considered in the previous section satisfy the whole set of Maxwell's equations (in particular $\rho = \rho_D = 0$), they are also solutions of the extended model. We can get new solutions by adding suitable stationary (not depending on time) fields \mathbf{E}_S and \mathbf{B}_S . This can be easily done if we assume that $\rho_S = \text{div}\mathbf{E}_S$ is constant (in particular we may choose $\rho_S = q$, for a given q). Thus, we set: $\mathbf{E} = \mathbf{E}_D + \mathbf{E}_S$, $\mathbf{B} = \mathbf{B}_D + \mathbf{B}_S$, $\rho = \rho_D + \rho_S = \rho_S = q$, $p = p_D + p_S$. In addition, we take \mathbf{V} as in (10). By plugging these expressions in (43)-(46), and recalling the relation (11), we must have:

$$c^2 \text{curl}\mathbf{B}_S = \rho_S \mathbf{V} \quad (51)$$

$$\text{curl}\mathbf{E}_S = (0, 0, 0) \quad (52)$$

$$\text{div}\mathbf{B}_S = 0 \quad (53)$$

$$\rho_S \left(\frac{D\mathbf{V}}{Dt} + \mu(\mathbf{E}_S + \mathbf{V} \times \mathbf{B}_S) \right) = -\nabla p_S \quad (54)$$

We can then come out with an explicit expression for \mathbf{E}_S and \mathbf{B}_S . We first note that:

$$\frac{D\mathbf{V}}{Dt} = -\frac{c^2\omega^2}{m^2} (r \sin^2 \theta, r \sin \theta \cos \theta, 0) = -\frac{c^2\omega^2}{2m^2} \nabla(r^2 \sin^2 \theta) \quad (55)$$

Successively, a possible choice for the stationary fields is:

$$\mathbf{E}_S = \frac{q}{3}(r, 0, 0) = \frac{q}{6}\nabla r^2 \quad \mathbf{B}_S = \frac{q\omega}{5mc} (-r^2 \cos \theta, 2r^2 \sin \theta, 0) \quad (56)$$

so that we get:

$$\mathbf{V} \times \mathbf{B}_S = -\frac{q\omega^2}{5m^2} (2r^3 \sin^2 \theta, r^3 \sin \theta \cos \theta, 0) = -\frac{q\omega^2}{10m^2} \nabla(r^4 \sin^2 \theta) \quad (57)$$

Let us observe that the magnetic field written above is exactly the one generated by a rotating sphere, uniformly charged (see e.g. [17], example 5.11). Putting all together we find out (see also (11)):

$$p = -\frac{\mu q}{m\omega}(rH' + H)S_2 \sin\theta \cos\zeta + \frac{c^2\omega^2 q}{2m^2}r^2 \sin^2\theta - \frac{\mu q^2}{6}r^2 + \frac{\mu\omega^2 q^2}{10m^2}r^4 \sin^2\theta \quad (58)$$

Other (singular) stationary fields compatible with the set of equations are the following ones (up to multiplicative constants):

$$\mathbf{E}_S = \left(\frac{1}{r^2}, 0, 0\right) \quad \mathbf{B}_S = \left(\frac{2\cos\theta}{r^3}, \frac{\sin\theta}{r^3}, 0\right) \quad (59)$$

In this case we get: $\text{div}\mathbf{B} = 0$, $\text{curl}\mathbf{B} = 0$, $\mathbf{V} \times \mathbf{B} = (c\omega/m)\nabla(r^{-1}\sin^2\theta)$ and $\rho_S = 0$. These last fields can be trivially incorporated in the pure Maxwellian part.

Some connections with the standard MHD can also be established. For example, our solution satisfies the *induction equation*:

$$\begin{aligned} \frac{\partial\mathbf{B}}{\partial t} &= \frac{\partial}{\partial t}(\mathbf{B}_D + \mathbf{B}_S) = \frac{\partial\mathbf{B}_D}{\partial t} = -\text{curl}\mathbf{E}_D \\ &= \text{curl}(\mathbf{V} \times \mathbf{B}_D) = \text{curl}[\mathbf{V} \times (\mathbf{B}_D + \mathbf{B}_S)] = \text{curl}(\mathbf{V} \times \mathbf{B}) \end{aligned} \quad (60)$$

where, in the order, we used that \mathbf{B}_S is stationary, and then (44), (11), (57). The literature on exact solutions in MHD is quite rich. We just mention a few references: [16], [30], [34]. The approach used in this paper is however rather original.

We conclude with some final remarks. A special subset of solutions (called *free-waves*) is obtained by simplifying (46) in the following way:

$$\mathbf{E} + \mathbf{V} \times \mathbf{B} = 0 \quad (61)$$

Thus, the Euler's equation will be trivially satisfied by setting: $D\mathbf{V}/Dt = 0$ and $p = 0$. In this case it is simple to deduce the orthogonality relations: $\mathbf{E} \cdot \mathbf{B} = 0$ and $\mathbf{E} \cdot \mathbf{V} = 0$. Moreover, we assume that the intensity of \mathbf{V} is constantly equal to the speed of light, i.e.: $|\mathbf{V}| = c$. If \mathbf{V} turns out to be the gradient of a potential function Ψ , we also get: $|\nabla\Psi| = c$, which is the stationary *eikonal* equation, ruling the dynamics of wave-fronts in geometrical optics. Hence, the revised set of equations strongly connects electrodynamics with classical optics, an important achievement that goes far beyond the usual Maxwell's model. It is also easy to check that free-waves satisfy the induction equation for an ideal conducting fluid, establishing another important link with MHD. In order to prove this, it is enough to take the curl of (61) and use (2).

Numerous examples of free-waves are available. Here, we just mention the following one in Cartesian coordinates (x, y, z) :

$$\mathbf{E} = \left(0, 0, cf(z)g(ct-x)\right), \quad \mathbf{B} = \left(0, -f(z)g(ct-x), 0\right), \quad \mathbf{V} = (c, 0, 0) \quad (62)$$

where f and g can be (almost) arbitrary. This wave solves (43), (44), (45), (61) and shifts at the speed of light along the x -axis. In general we have $\rho \neq 0$. Imposing $\rho = 0$ implies that f is a constant function, showing that parallel wave-fronts of Maxwell's type ($\text{div}\mathbf{E} = 0$) can only be plane-waves of infinite extension. Instead, if f and g have a prescribed bounded support and vanish at its boundary, the wave remains constrained in a shifting portion of space. As we already said, the continuity equation is automatically satisfied.

7 Speculations about the constitution of the Sun and the solar system

Since the pioneering papers of H. Alfvén (see e.g. [2]), the study of the evolving plasma in the heliosphere is a widely investigated subject. Moreover, the role of plasma is recognized to be a primary factor to understand our universe at all scales of magnitude (see e.g. [27], [28]). The EM environment introduced in the previous sections may represent a possible background distribution, in support of more complex phenomena. If such a guess is correct, we can come out with some interesting observations.

Actually, we begin with advancing some conjectures about our Sun. We refer to the circular electric patterns of Fig. 3. Assuming that the *solar cells* have an averaged diameter $d = 1100$ Km, there are about $2\pi R_\odot/d \approx 4000$ of them along the equatorial circumference (R_\odot being the Sun radius). This means that $m \approx 2000$. We can choose ℓ in such a way that $\ell/m \approx 2$. With this choice, the number of cells lined up along the equator is approximately equal to those lined up along a meridian. Roughly, the Bessel's function $J_\alpha(r)$ has its first positive root for $r \approx \alpha$. The function is practically zero, presenting a sudden bump just before such a root. This says that the cells have a relatively small depth. In the case of $J_{\ell+1/2}(\omega r)$ (see (22)), we then get $\omega \approx \ell/R_\odot$. According to (10), the intensity of \mathbf{V} on the equator is $|\mathbf{V}| = c\omega R_\odot/m \approx c\ell/m \approx 2c$. Therefore, this final result is almost independent of all the parameters, with the exception of c . We recall that c appears in the wave equations (5).

The solar sphere is a medium containing material particles, whose movement is accompanied by their EM interactions. Particles supply the EM field in their motion and, at the same time, they are dragged by a mechanism related to Lorentz's force. Due to the fact that they are massive, the velocity constant c should be suitably reduced, by arguing that the medium intrinsically presents a relative dielectric constant higher than that of vacuum, forcing the information described by \mathbf{V} to evolve at lower velocities. A quantitative analysis (too technical for the purpose of this paper) involves the knowledge of the electrical conductivity σ of the Sun (see e.g. [36], section 8.1.2). If c is the speed of light in vacuum, a period of rotation around the vertical axis, turns out to be approximately 4.65 seconds. This is 16×10^3 times smaller than the revolution period of the Sun of about 27 days. Thus c must be reduced accordingly.

We can provide an alternative explanation. Instead of adapting the value of c

to the conductive characteristics of the solar plasma, we can continue to suppose that c is the speed of light in vacuum. Therefore, there is a high-frequency pure EM wave turning around that acts as a forcing term. Such a wave may be rather simple as in Fig. 4. As charged particles are present, they are dragged into a rotatory motion, but they do this by following patterns that are strictly related to various physical quantities, such as: the intensity of the charges involved, their masses, their density within the plasma. The slower global motion is a consequence of the above restrictions, whereas the EM information still develops at its classical speed. This viewpoint stimulates a further conjecture. A star is formed when, due to the creation of a swirl in the EM background (like a tornado in air), preexisting particles glue together (by electro-dynamical and gravitational forces) conferring stability to the newborn structure and finding a state of dynamical equilibrium. We also observe that vortexes of electric type on the solar surface may give raise to magnetic loops (*spicules*), as a trivial consequence of Faraday's law. These filaments, that can carry particles as well, ignite the mechanism at the origin of solar flares. Of course, our construction is elementary if compared to the complexity of a star. On the other hand, we are just building our assumptions based on the solutions of linear problems.

Outside the massive bulk of the star we still have plasma, but with an extremely small concentration of particles. We are basically in vacuum so that the information now really evolves at speeds comparable to that of light. By this we do not mean that particles necessarily travel fast. It is the flow of EM information in which they are embedded in that develops at luminous velocities.

The Sun has several ways to let us know its presence. First, it emits photons. These tiny energy packets escape as a consequence of chemical or subatomic reactions. They carry away EM energy and they are fully described by the model equations of section 6 (see the fields expressed by (62)), and, incidentally, also solve the MHD equations. Photons constitute the visible part, since they can be detected with our eyes or instruments. We claim that there is another mean, only indirectly observable, used by the Sun to leave fingerprints on the surrounding space. The turbulent EM status of the star induces the creation of complicated (but well organized) whirls and spirals as described in section 5. This process generates a sequence of encapsulated shells, whose size reasonably grows geometrically. Inside each shell there are trapped EM waves, coordinately traveling and performing a peculiar dance. The transition between a shell and the next one happens with continuity. Differently from [9], we have shown here that it is possible to connect the different domains by avoiding shocks on the magnetic fields. We also assumed that the interfaces are surfaces displaying zero magnetic field, though this hypothesis may be reviewed at the occurrence. These systems evolve at an averaged speed comparable to that of light. As they become larger, the angular velocity diminishes. We also observe that rotating EM solutions constrained in finite regions of space are well suited for domains having annular topology ([8], [13], [15]). This may suggest developments based on other geometries. In reality, changes in the magnetic field have been detected by interplanetary probes. Some theories have been consequently developed (see [35], [6], [7]). Quick intermittent magnetic reversals in proximity of the Sun

have been also reported (see for instance: [18], [5], [21]).

Thus, according to our viewpoint, there is an organized set of shells which is not directly visible. We can however appreciate its existence in indirect way. Perhaps, this construction may contribute to explain the formation of planets, initially in a state of fragments (*planetesimals*) and successively compacted by self-gravity and the action of an organized plasma (see e.g. [2], [3]). The EM storms surrounding the Sun, force the selection of distant regions of space where bunches of wrecks may meet and join together. Indeed, the analysis of the first modes involved in the construction of the external shells (consider the case $m = \ell$ examined in section 5) says that a privileged direction is that of the equatorial plane. This suggests a possible explanation of the (almost) coplanar distribution of the planets. Moreover, it seems that there are more chances to find matter in zones where the interface magnetic field vanishes. Indeed, according to [20], charged particles actually tend to accumulate in regions where the magnetic field is of weakest strength. Due to the geometrical growth of the shells, we can advocate for the existence of specific spots where it is more likely to find planets. This turns out to be in agreement with the Titius-Bode law, in which the averaged distance of the planets from the Sun follows a geometric growth rate: $.4 + .3 \times 2^k$, where the unity of measure of the distance is expressed in AU. Note that in the right picture of Fig. 5, the ratio r_{\max}/r_{\min} is actually very close to 2.

Finally, we would like to emphasize another aspect of the construction here proposed. The solutions may actually contain a dynamical part plus a stationary one (or pseudo-stationary, by meaning that this develops at speeds that are much lower than that of light). We illustrated how this can be done in section 6 with the fields, $\mathbf{E} = \mathbf{E}_D + \mathbf{E}_S$, $\mathbf{B} = \mathbf{B}_D + \mathbf{B}_S$, although we do not have more fancy analytic expressions to show. Thus, the EM activity at the exterior of the Sun can be enriched by the addition of pseudo-stationary components. In this way we simulate a kind of *solar wind*, developing with continuity across the various layers. The line of force corotate with the Sun and may be either closed or open loops depending on the distance (see [10], [31]). To this extent, we characterize the idea of a *Parker's spiral* (see [26]), as a further message imprinted on the plasma. Exact solutions of this type, in the context of MHD, are given for instance in [4]. A laboratory recreation of a spiraling wind, through a rapidly rotating plasma magnetosphere, has been achieved in [29]. Analytic solutions for the spiraling fields generated by a rotating magnetic dipole are given in [33].

Similar constructions can be applied to satellites. Indeed, each planet is expected to be surrounded by an EM environment similar to that studied so far. Such an alteration comes into conflict with that of the Sun, producing a deviation of the solar wind and the reconnection of the magnetic streamlines along alternative patterns (see e.g. [32]). Changes in the Earth magnetic field are documented since long time (see e.g. [11]). They occur with variable periods (daily, seasonal, secular). The consequence of our reasoning is that our planet, during the travel along its orbit, is at the mercy of complex preexisting periodic EM recurrences filling up the whole heliosphere (see [24], [25]). We stop however our exposition at this point. A deeper analysis on these issues would bring us

too far from the limits we fixed for this paper.

References

- [1] Abramowitz M., Stegun I. A. (Eds.), *Handbook of Mathematical Functions with Formulas, Graphs and Mathematical Tables*, Applied Mathematics Series, 55, Dover Publications, 1965.
- [2] Alfvén H., *On the Origin of the Solar System*, Clarendon Press; 1st Edition, 1954.
- [3] Alfvén H., Cosmology in the plasma universe: An introductory exposition, *IEEE Trans. on Plasma Science*, **18** (1990), 5-10.
- [4] Asghar S., Khan M., Siddiqui A. M., Hayat T., Exact solutions for magneto-hydrodynamic flow in a rotating fluid, *Acta Mechanica Sinica*, **18**, 3 (2002), 244-251.
- [5] Bale S. D. et al., Highly structured slow solar wind emerging from an equatorial coronal hole, *Nature*, **576** (2019), 237-242.
- [6] Burlaga L. F., Directional discontinuities in the interplanetary magnetic field, *Solar Phys.*, **7** (1969), 54-71.
- [7] Burlaga L. F. et al., Magnetic field and particle measurements made by Voyager 2 at and near the heliopause, *Nature Astronomy*, **3** (2019), 1007-1012.
- [8] Chinosi C., Della Croce L., Funaro D., Rotating electromagnetic waves in toroid-shaped regions, *Int. J. Modern Phys. C*, **21**, 1 (2010), 11-32.
- [9] Colburn D. S., Sonett C. P., Discontinuities in the Solar wind, *Space Science Reviews*, **5** (1966), 439-506.
- [10] Ferraro V. C. A., Bhatia V. B., Corotation and solar wind in the solar corona and interplanetary medium, *Astrophysical J.*, **147** (1967), 220-229.
- [11] Fleming J. A., Time-changes of the Earth's magnetic field, *The Scientific Monthly*, **34**, 6 (1932), 499-530.
- [12] Funaro D., *Electromagnetism and the Structure of Matter*, World Scientific, Singapore, 2008.
- [13] Funaro D., Trapping electromagnetic solitons in cylinders, *Math. Model. and Anal.*, **19**, 1 (2014), 44-51.
- [14] Funaro D., *From Photons to Atoms, The Electromagnetic Nature of Matter*, World Scientific, Singapore, 2019.
- [15] Funaro D., Electromagnetic waves in annular regions, *Applied Sciences*, MDPI, **10**, 5 (2020), 1780.
- [16] Golovin S. V., Dudnik M. N., Unsteady flows with a constant total pressure described by the equations of ideal magnetohydrodynamics, *J. Appl. Mech. Tech. Phys.*, **55**, 2 (2014), 234-246.

- [17] Griffiths D. J., *Introduction to Electrodynamics*, 3rd Edition, Prentice Hall, 2007.
- [18] Horbury, T. S. et al., Short, large-amplitude speed enhancements in the near-Sun solar wind, *Mon. Not. R. Astron. Soc.*, **478** (2018), 1980-1986.
- [19] Jackson J. D., *Classical Electrodynamics*, 2nd Edition, John Wiley & Sons, 1975.
- [20] Karsten J., Pogolian L., Relieving the Hubble tension with primordial magnetic fields, *Phys. Rev. Lett.*, **125** (2020), 181302.
- [21] Kasper J. C. et al., Alfvénic velocity spikes and rotational flows in the near-Sun solar wind, *Nature*, **576** (2019), 228-231.
- [22] Landau L.D., Lifschits E. M., *The Classical Theory of Fields*, 3rd Ed., Pergamon Press, 1971.
- [23] Longuet-Higgins M. S., The eigenfunctions of Laplace's tidal equations over a sphere, *Phil. Trans. Royal Soc. London, Series A, Math. and Phys. Sci.*, **262**, 1132 (1968), 511-607.
- [24] McPherron R. L., Magnetic pulsations: their sources and relation to Solar wind and geomagnetic activity, *Surveys in Geophysics*, **26** (2005), 545-592.
- [25] Milan S. E. et al., Overview of Solar wind-magnetosphere-ionosphere-atmosphere coupling and the generation of magnetospheric currents, *Space Science Reviews*, **206** (2017), 547-573.
- [26] Parker E. N., Dynamics of the interplanetary gas and magnetic fields", *Astrophys. J.*, **128** (1958) , 664.
- [27] Peratt A. L., Plasma Cosmology, *Sky & Tel.*, Feb. 1992, 136.
- [28] Peratt A. L., *Physics of the Plasma Universe*, 2nd Edition, Springer, NY, 2015.
- [29] Peterson E. E. et al., A laboratory model for the Parker spiral and magnetized stellar winds, *Nature Phys.*, **15** (2019), 1095-1100.
- [30] Picard P. Y., Some exact solutions of the ideal MHD equations through symmetry reduction method, *J. Math. Anal. Appl.*, **337** (2008), 360-385.
- [31] Pneuman G. W., Kopp R. A., Gas-magnetic field interactions in the solar corona, *Solar Phys.*, **18** (1971), 258-270.
- [32] Priest E., Forbes T., *Magnetic Reconnection*, Cambridge Univ. Press, 2000.
- [33] Sarychev V., Electromagnetic field of a rotating magnetic dipole and electric-charge motion in this field, *Radiophysics and Quantum Electronics*, **52**, 12 (2009), 900-907.
- [34] Shokri M., Sadooghi N., Novel self-similar rotating solutions of non-ideal transverse magnetohydrodynamics, *Phys. Rev. D*, **96** (2017), 116008.

- [35] Siscoe G. L., Davis L. Jr., Coleman P. J. Jr., Smith E. J., Jones D. E., Power spectra and discontinuities of the interplanetary magnetic field: Mariner 4, *J. Geophysical Res.*, **73**, 1 (1968), 61-82.
- [36] Stix M., *The Sun, An Introduction*, Springer, 1989.
- [37] Wang H., Boyd J. P., Akmaev R. A., On computation of Hough functions, *Geosci. Model Dev.*, **9** (2016), 1477-1488.